Available online at www.sciencedirect.com
ScienceDirect
Ceramics International 35 (2009) 861–868
CERAMICS INTERNATIONAL
www.elsevier.com/locate/ceramint

Atmosphere and carbon effects on microstructure and phase analysis of *in situ* spinel formation in MgO–C refractories matrix

M. Bavand-Vandchali *, H. Sarpoolaky, F. Golestani-Fard, H.R. Rezaie

Department of Metallurgical and Material Engineering, Iran University of Science and Technology (IUST), PO Box 16846-13114, Narmak, Tehran, Iran

Received 27 August 2007; received in revised form 19 January 2008; accepted 7 March 2008
Available online 1 July 2008

Abstract

The effects of carbon, air and reducing atmospheres on microstructure and phase evolution of *in situ* $MgAl_2O_4$ spinel (S) formation in the matrix of MgO–C refractories were investigated by X-ray diffraction powder analysis (XRD) and scanning electron microscopy (SEM)/energy-dispersive spectroscopy (EDS) techniques. The formation of spinel started under 1000 °C in both air and reducing atmospheres. The morphology of *in situ* spinel and its formation mechanism were however different and dependent upon the atmosphere. The solid-state reaction was clarified to be the dominant mechanism of spinel formation in oxide atmosphere, while the gas–solid reaction was found to play a vital role in reducing atmosphere. Reaction of MgO and C in reducing atmosphere led to the formation of $Mg_{(g)}$ which was found to be partially controlling the *in situ* spinel formation in the carbon containing samples fired in reducing environment. The results which were necessary are explained with emphasis on MgO–C refractories applications.

Keywords: $MgAl_2O_4$ spinel; MgO–C refractories; Reactive alumina; Microstructure

1. Introduction

Spinel (S) group minerals have mixed oxide structure with chemical formula of $RO\text{-}R'_2O_3$ (where R and R′ are a wide range of divalent and trivalent metal elements, respectively), which have been widely used as ceramic materials due to their particular properties. Magnesium aluminate (MA) spinel is the only stable compound in $MgO–Al_2O_3$ binary system, showing a wide range of non-stoichiometry compositions by solution of MgO and Al_2O_3 in its structure at high temperature. MA spinel is also used extensively as a refractory material because of its high-melting point and suitable high-temperature properties [1,2].

MA spinel containing refractories are increasingly popular due to their exceptional behavior in several applications especially in metallurgical and other high-temperature process industries [3,4]. The outstanding high-temperature mechanical, chemical and thermal properties of spinel are the reasons for increasing of MA spinel application in refractories. Therefore, presence of spinel in the matrix of refractories can improve thermal shock resistance and corrosion behavior of the products [5]. Spinel is also a beneficial phase formed at high temperatures in magnesia–carbon refractory materials containing metals or alloys (Al, Al/Si, Al/Mg) as antioxidant [6]. Recently, use of *in situ* spinel in the matrix of MgO base refractories and its effects on properties have become of great importance. In this regards, reactive alumina addition to MgO–C refractories has been developed because of its benefits on spinel formation, microstructure integrity and improvement of thermo-chemical properties [7].

The direct reaction of magnesia and alumina to form MA spinel is accompanied by a volume expansion of approximately 5% [8,9]. Therefore, this expansion can be beneficial to the healing of thermal stress cracks or an improved resistance to slag corrosion for MA spinel containing refractories that used in industrial applications [10]. Also increased interest in the concept of *in situ* formed MA spinel has directed efforts to seek more economical production approaches for these kind of refractories [11].

Microstructural evolution in refractory materials is particularly important due to their multi-phase nature and critical

* Corresponding author. Tel.: +98 21 88886740; fax: +98 21 88886726.
E-mail address: Mbavand@iust.ac.ir (M. Bavand-Vandchali).

0272-8842/$34.00
doi:10.1016/j.ceramint.2008.03.001

Table 1
Chemical composition of raw materials

	MgO	C	CaO	SiO_2	Al_2O_3	Na_2O	Fe_2O_3
Fused magnesia	97	–	1.2	0.5	0.2	–	0.4
Sintered magnesia	97.5	–	1	0.5	0.5	–	0.6
Graphite flake	0.13	96.5	0.13	1.6	0.45	–	0.75
Reactive alumina (ppm)	–	–	150	800	99.5	350	150

effects of final microstructure on properties and corrosion behavior. Also, the control of phase transformations in the refractories microstructure is a key issue in their behavior in practice. For a full understanding of the final microstructure of a refractory system, it is strictly necessary to characterize the microstructures after each firing step. It is also important for a special type of refractories so-called *in situ* refractories that new phases were formed in the microstructure during firing process on operation. However, much useful information can be obtained by examining the microstructure at different temperatures [12].

The purpose of the present study was to evaluate the microstructure and phase analysis of *in situ* spinel formation in the matrix of MgO–C refractories containing fine reactive alumina powders regarding to the sintering atmosphere and carbon presence.

2. Experimental procedures

High quality commercial chinese fused and sintered magnesia powders, chinese natural flake graphite (G) and reactive alumina powder additive ($d_{50} = 2.5$ μm) (Pechiney Co., France) with chemical composition according to Table 1 were used as primary materials. To investigate the influence of carbon and atmosphere on *in situ* spinel formation, two types of samples were prepared according to the matrix of MgO–10% C refractory. Therefore, the batches were prepared with oxide aggregates smaller than 200 μm. All starting powders were weighted and mixed according to Table 2, pressed at 150 MPa in a stainless steel die with 20 mm diameter and a thickness of 10 mm. Two kinds of atmosphere namely carbon bed (reducing) and air (oxidizing) were employed for firing samples at 1000–1700 °C with a rate of 10 °C/min and 3 h dwell. Sample containing graphite was labeled as MRC (Table 2) only fired at reducing atmosphere and graphite free samples with similar oxide compositions were fired at reducing and oxidizing atmospheres, which were labeled as MRR and MRO, respectively (Table 2). The samples were characterized in terms of microstructure and phase analysis after firing. For X-ray diffraction powder analysis (XRD), the samples were crushed and sieved (<50 μm) and diffractograms recorded on a Philips PW1050 unit using Cu Kα radiation operating at 30 mA and 40 kV. Samples for microstructural analysis were taken from center of fired billet and impregnated with resin, ground, polished and then gold-coated using standard ceramographic techniques. Because of the unsuitable strength in samples fired at low temperatures, microstructure observations only were carried out in samples fired at high temperature. A scanning electron microscopy (SEM) (Philips, XL30, Nederland) equipped with an energy-dispersive spectroscopy (EDS) analyzer was used for back scattered electron imaging (BSI).

Table 2
Chemical compositions of samples and firing atmosphere

Materials	Sample code		
	MRC	MRR	MRO
Fused magnesia, <150 μm	50.40	56.0	
Sintered magnesia, <75 μm	13.68	15.2	
Graphite flake, <150 μm	10.00	–	
Reactive alumina	25.92	28.8	
Firing atmosphere	Carbon bed	Carbon bed	Air

3. Results and discussion

Microstructure and phase analysis of *in situ* spinel formation in the matrix of MgO–C refractories were investigated in terms of oxidizing, reducing atmospheres and presence of carbon influences.

3.1. In situ spinel formation in oxide atmosphere

Fig. 1 shows the XRD patterns of MRO sample fired at different temperatures in oxidizing atmosphere. The presence of MA spinel was detected from initial firing temperature (1000 °C) and its peaks intensity increased steadily with firing temperature. Spinel and periclase were identified as principle crystalline phases after firing at 1450 °C, while corundum content decreased rapidly with increasing temperature and disappeared above 1450 °C. In XRD patterns the small peaks attributed to merwinite ($3CaO{\cdot}MgO{\cdot}2SiO_2$, C_3MS_2) could also be identified. It is well known that merwinite as a low-temperature phase is originated from MgO impurities and usually locates at grain boundaries of periclase crystals [13]. Since the above-mentioned peaks were also present in XRD pattern of primary chinese dead-burned magnesia, we may conclude that the existing merwinite phase comes from raw

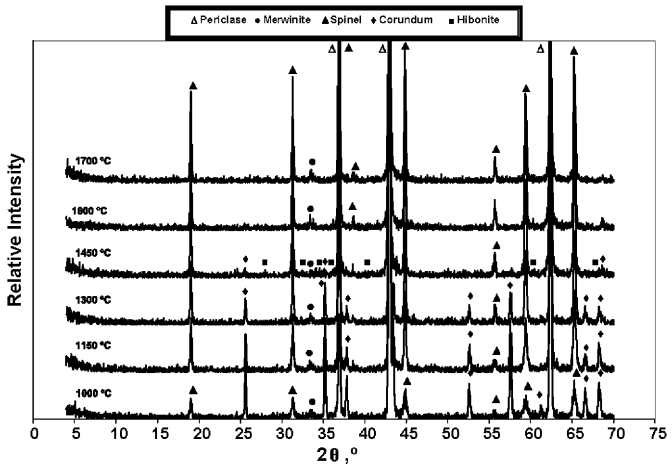

Fig. 1. XRD patterns of MRO sample fired at different temperature and oxide atmosphere.

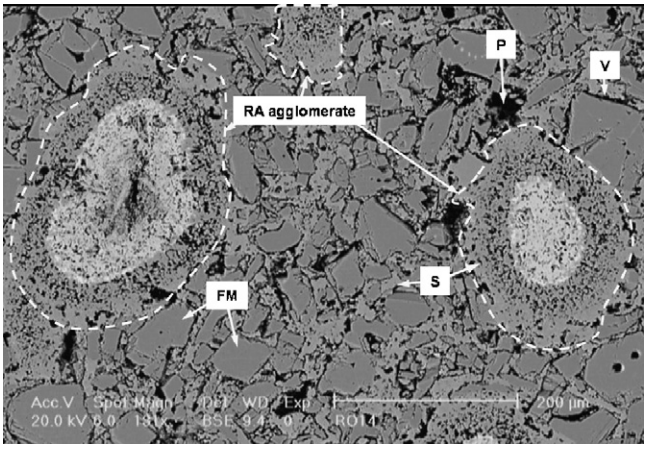

Fig. 2. SEM micrograph of MRO sample fired at 1450 °C showing the different sizes of halos in the texture. RA: reactive alumina; FM: fused MgO; S: spinel; V: void; P: pore.

materials. Careful study of the XRD pattern at 1450 °C also clarified traces of calcium hexa-aluminate ($CaO{\cdot}Al_2O_3$, CA_6 or Hibonite). This compound is usually formed by reaction of Al_2O_3 with small amount of CaO that might be originated from impurities present in magnesia grins.

A typical microstructure of MRO sample fired at 1450 °C (Fig. 2) revealed magnesia grains (FM) surrounded by spinel matrix throughout the whole sample. The spinel matrix, of course, is formed by reaction of MgO fine grains and alumina powders. Also, in this micrograph the rather large white halo surrounded by a porous area are observed. These types of white halos were formed to be spread in the microstructure and their sizes were in the range of 100–300 μm approximately.

The halo with 300 μm in size is observed in higher magnification in Fig. 3a. As shown, the halo is composed of three layers with different morphologies and contrasts and the qualitative analysis of the above three layers by EDS revealed different compositions (Fig. 3b). The alumina is present in all three layers analysis while calcia and magnesia are detected in middle and surface layers, respectively. Quantitative chemical analysis of layer 1 revealed a weight ratio of 75/24 for Al_2O_3/MgO, which is an indication of near stoichiometric MA spinel composition. Looking at layer 2 in higher magnification demonstrated a needle-like texture, as shown in Fig. 4. The EDS analysis showed a weight ratio of 85/15 for Al_2O_3/CaO, which is well compared to reported alumina rich calcium hexa-aluminate (CA_6) [3]. In layer 3 only alumina was analyzed by EDS and therefore it is most probable that this layer consist of un-reacted primary reactive alumina particles.

Fig. 5a shows another halo type phase with size of nearly 200 μm, which consists only two layers. The white central area was analyzed as CA_6 and the surrounding grey area was found to be spinel. The interface between two above layers was also shown in Fig. 5b. As seen in addition to calcium hexa-aluminate and spinel another phase in white contrast can be distinguished where CA_6 and spinel meet each other. The EDS analysis of this phase revealed the calcium aluminium silicate ($CaO.Al_2O_3.SiO_2$, calcium alumina silicate (CAS)) composition with small amounts of MgO that is likely liquid at 1400 °C [14]. Looking through the scanning electron microscopy microstructure we also identified small halos with max. size 100 μm consisted of only one area as seen in Fig. 6. The EDS analysis of this layer showed the MA spinel composition.

The above-mentioned observations clarified the presence of alumina agglomerates with sizes of 100–300 μm in diameter. It seems that such agglomeration of reactive alumina powders can be attributed to mixing process where the fine reactive particles due to high tendency to agglomerate, combine and behave in microstructure as a large alumina particles. During the firing,

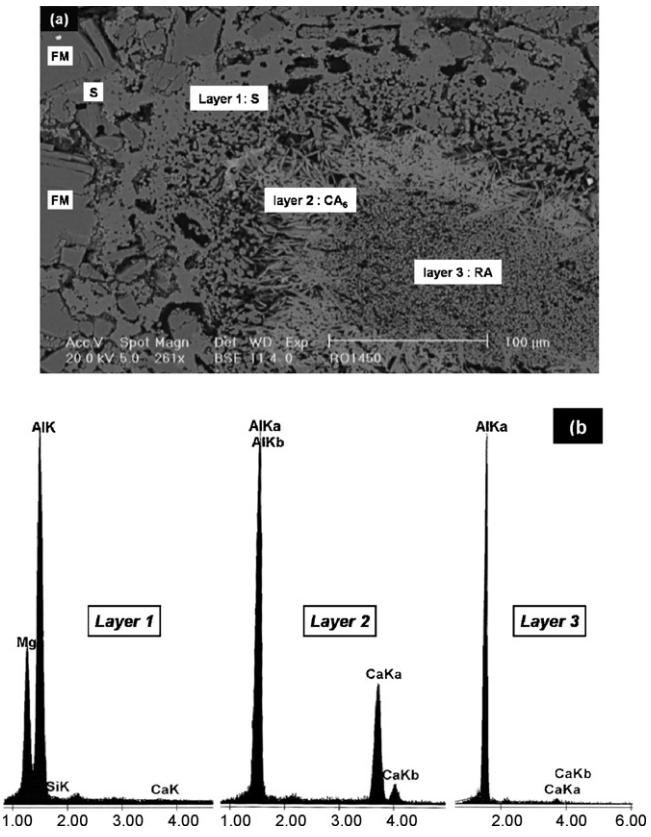

Fig. 3. SEM micrograph of MRO sample fired at 1450 °C showing the three layers in a large halos (a). The EDS analysis of the layers 1–3 (b). FM: fused MgO; S: spinel; RA: reactive alumina.

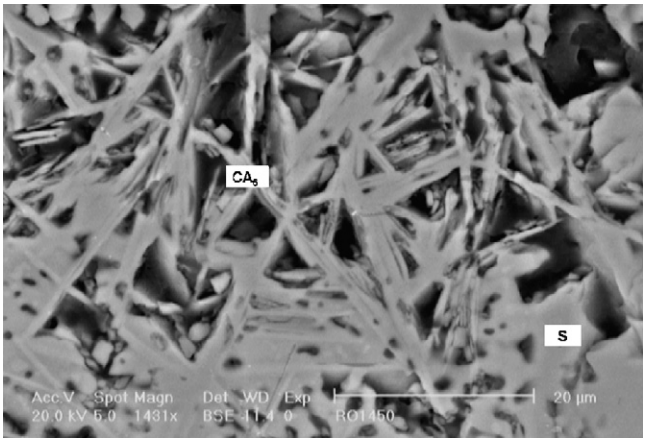

Fig. 4. Formation of CA_6 whisker crystals in layer 2 of large halos in Fig. 3. S: spinel.

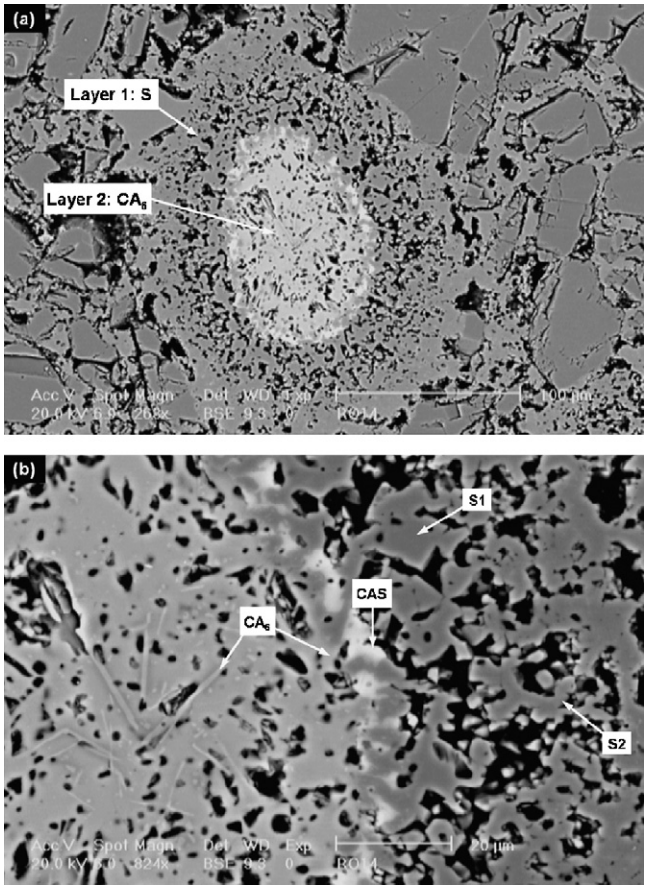

Fig. 5. SEM micrograph of the MRO sample fired at 1450 °C: (a) formation of two layers in medium size halos and (b) interface of layers 1–2. S: spinel; S1: angular shape spinel; S2: tuber-like spinel.

these alumina particles start the reaction with surrounding MgO grains to form primary spinel.

The spinel formation in the mixture of alumina and magnesia could be understood by the Wagner theory [15]. It has been clarified that the *in situ* spinel formation during the firing process in the $MgO–Al_2O_3$ system is controlled by counterdiffusion of Mg^{2+} and Al^{3+} ions through the formed spinel layer. Also, the diffusivity of Mg^{2+} ions and reactivity of alumina are plying important role on the rate of *in situ* spinel formation [16]. The agglomeration and fast densification of reactive alumina decrease its reactivity and slow down the formation of spinel. Particularly in the center of alumina agglomerates, the particles remain far from surrounding magnesia and therefore un-reacted. However, as shown in Figs. 1–3, all there well-dispersed reactive alumina in the matrix completely reacted with finer MgO grains and formed a continuous spinel matrix in the texture.

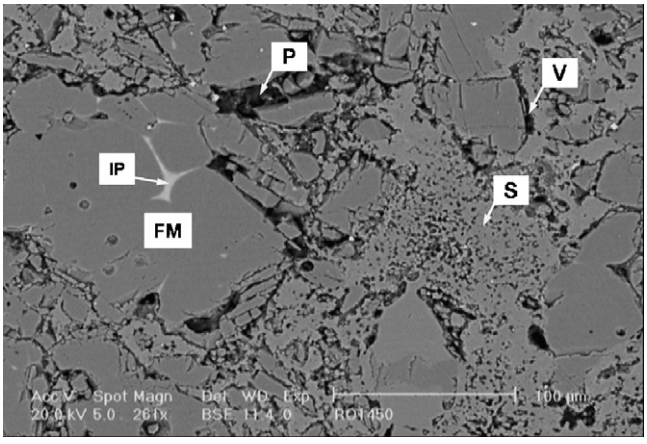

Fig. 6. SEM micrograph of the MRO sample fired at 1450 °C showing the one layer in small halos. FM: fused MgO; S: spinel; V: void; P: pore; IP: impurity phase.

On the basis of above-mentioned mechanism, the large agglomerates would convert into three layers textures after firing at 1450 °C. The smaller agglomerates, however, the layers would decrease and either of the central alumina or the middle calcium hexa-aluminate in large and middle agglomerates would disappear due to reaction completion.

The CA_6 formation on the MgO/agglomerate interface can be attributed to the reaction of CaO and alumina. In fact, the CaO existing in calcium silicate phases present in the magnesia (such as merwinite, C_3MS_2) migrate towards alumina in the direction of alumina agglomerates center. Despite the presence of Mg^{2+} and Si^{4+} ions the higher diffusion coefficient of Ca^{2+} ions encourage the formation of calcium aluminate phases prior to spinel formation, which has been started to form at lower temperatures. The diffusion coefficients of cations in the silicate melts has been reported in the following order: $D_{Ca} \geq D_{Mg} \gg D_{Si}$ [17]. The amount of calcium aluminate phases and its morphology were also clarified, which related to diffusion rate of Ca^{2+} ions, size and level of porosity in the reactive alumina agglomerates [18].

It was also clarified that the morphology of *in situ* spinel is a complex function of many factors including local composition and temperature [14,15]. Therefore, consistent with the present work the different morphology of *in situ* formed spinel including angular/facetted crystals (labeled S1 in Fig. 5b) and tuber-like (S2 in Fig. 5b) might be originated due to presence of calcium alumina silicate (CAS) liquid phase.

The backscattered SEM image of the MRO sample fired at 1600 °C (Fig. 7a) revealed the existence a hollow space in the center of original agglomerates. It seems that two coexisting process of sintering shrinkage of reactive alumina particles and expansion nature of spinel formation are causing the hollow creation. It is interesting that the hollow shape is observed almost in all agglomerates regardless of their sizes. The similar mechanism on the formation of hollow spinel has been also reported by previous researchers [15,16]. Many voids (V) or mismatch gaps were also observed around the MgO grains and separated them from the spinel matrix (Fig. 7b). This texture generally was formed during cooling because of the difference of thermal expansion coefficients between MgO and spinel. The microstructure of MRO sample fired up to 1700 °C shows the relatively dense structure due to promotion of sintering and hollow spots remained from agglomerates (Fig. 8a).

At higher magnifications (Fig. 8b), the microstructure of formed spinel shows the presence of bright phase trapped in triple junction of spinel crystals. The EDS analysis of these bright phases showed the compositions of $CaO–MgO–Al_2O_3–$

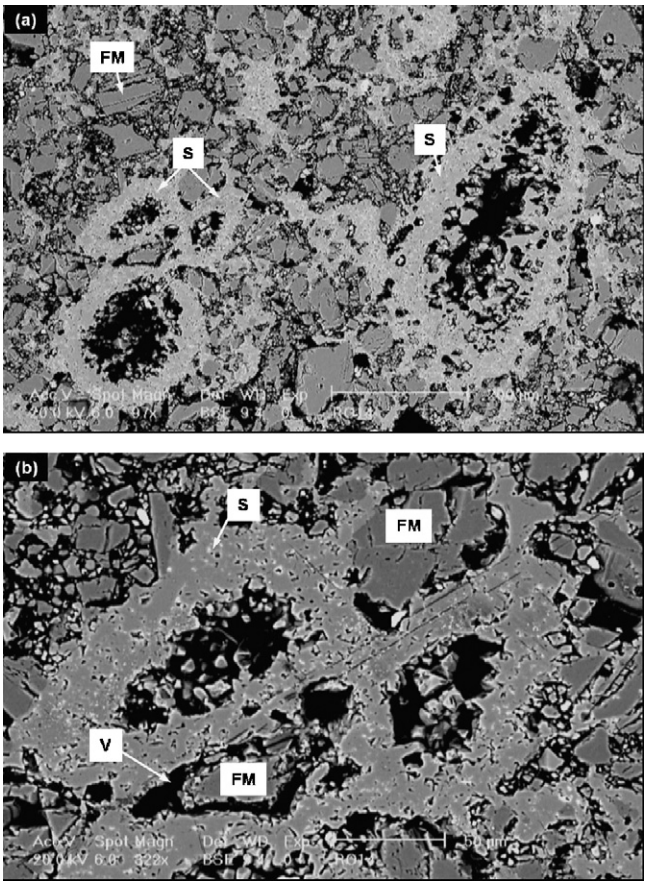

Fig. 7. SEM micrograph of the MRO sample fired at 1600 °C showing the formation of hollow grains in two magnification. FM: fused MgO; S: spinel; V: void.

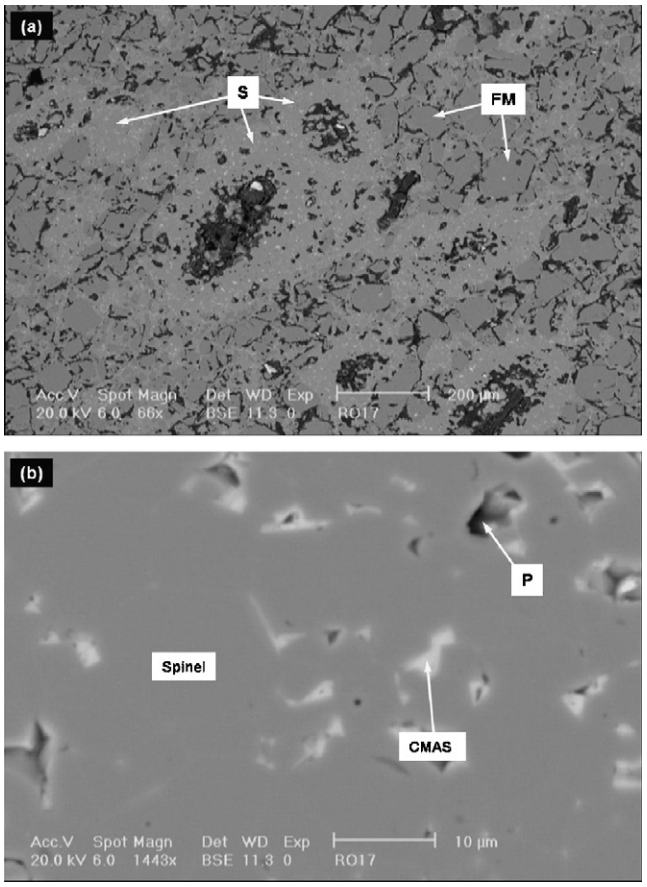

Fig. 8. SEM micrograph of the MRO sample fired at 1700 °C (a), high magnification of spinel texture (b). FM: fused MgO; S: spinel.

SiO_2 oxides, which probably are liquid at 1600 °C [14]. The formation of the above CMAS phases can be attributed to reaction of MgO impurities and alumina at high temperatures which has been reported before [18,19].

3.2. In situ spinel formation in reducing atmosphere and presence of carbon

Fig. 9 shows the XRD patterns of MRC sample fired at different temperatures in reducing atmosphere. Similar to MRO sample, the spinel phase was formed below 1000 °C and its intensity increased by raising the firing temperature. However, the intensity of corundum peaks decreased inversely to spinel and disappeared at 1450 °C. The periclase, graphite and spinel were the main phases above 1450 °C. The phase analysis of fired MRR sample (not shown) also revealed the similar trend in formation of spinel and disappearing of corundum, while the periclase and spinel were the principle phases above 1450 °C.

A typical micrograph of MRC sample fired at 1600 °C in reducing atmosphere was shown in Fig. 10. The MgO grains and flake graphite were dispersed homogeneously in the network of spinel matrix. Unlike MRO sample fired at 1600 °C (Fig. 7), solid halos (S) with white contrast are observed in the texture of MRC samples. The EDS analysis of these condensed halos showed the composition of near stoichiometric MA spinel. Therefore, it can be concluded that these large spinel grains are the initial alumina agglomerates that reacted with surrounding MgO grains by firing at 1600 °C. The relative high amount of reactive alumina and presence of graphite flakes can increase the formation of agglomerates in MRC sample. The higher magnification showed that no hollow space was present in the center of solid spinel grains (on the contrary to MRO sample) (Fig. 11a). The formation of spinel network was also revealed in the matrix. Fig. 11b illustrate higher magnification

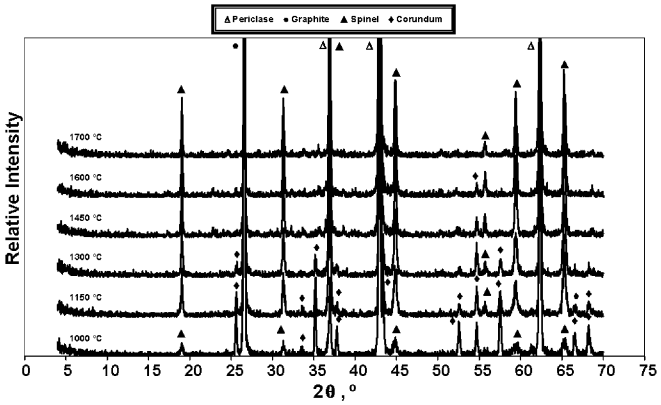

Fig. 9. XRD patterns of MRC sample fired at different temperature and reduced atmosphere.

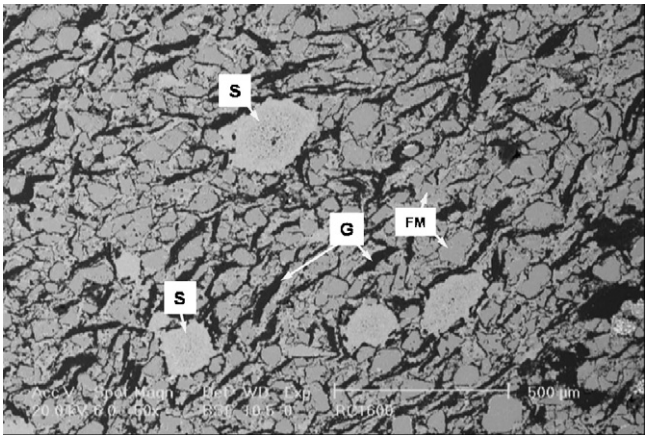

Fig. 10. SEM micrograph of the MRC sample fired at 1600 °C showing the formation of solid halos in the texture. FM: fused MgO; S: spinel; G: graphite.

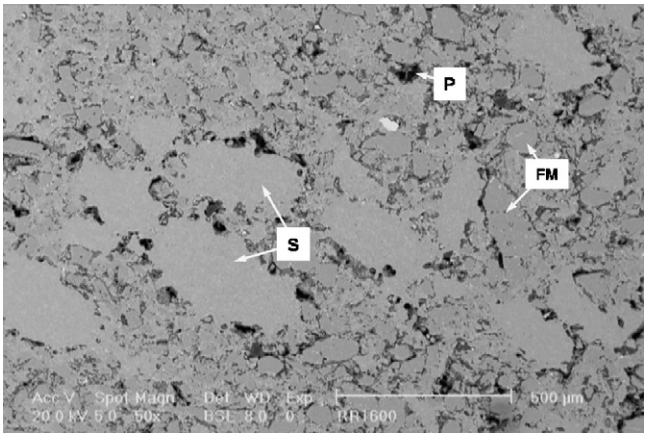

Fig. 12. SEM micrograph of the MRR sample fired at 1600 °C showing the formation of dense spinel grains. FM: fused MgO; S: spinel; P: pore.

of the *in situ* spinel network that is formed between MgO–MgO grains and MgO–graphite flakes with no apparent voids in the matrix. This interlocking texture of *in situ* spinel is accompanied by structural integrity that can be used to interpret of the corrosion behavior in graphite containing refractories. Generally, oxidation of carbon and subsequent dissolution of MgO grains in the molten slag are the two main factors that are considered to be responsible for the corrosion of MgO–C refractories. Furthermore, it is well known that the presence of carbon can improve the wear resistance of oxide-based refractories [20]. Therefore, it can be concluded that the development of continuous spinel bond can hold graphite flakes in the matrix and subsequently lead to higher corrosion resistance of MgO–C refractories. This also maintained the strengthening of the refractory texture and thus improved the physical/mechanical properties [5,21].

A typical microstructure of MRR sample fired in reducing atmosphere at 1600 °C (Fig. 12) also showed the presence of MgO grains surrounded by a continuous spinel matrix. The different size of solid spinel grains were also observed in the microstructure similar to the MRC sample (Fig. 10). Many voids were seen between MgO grains (SM) and formed spinel matrix as same as MRO sample (Fig. 13).

The microstructure of MRC and MRR samples at 1700 °C had the similar nature as 1600 °C. Fig. 14 shows the texture of solid spinel grains where the bright phases were formed at the triple junctions of spinel crystals. The qualitative EDS analysis revealed the CMAS compositions, which are liquid at 1500 °C.

In spite of microstructural features and formation of hollow spinel in MRO sample, the solid spinel grains were observed in

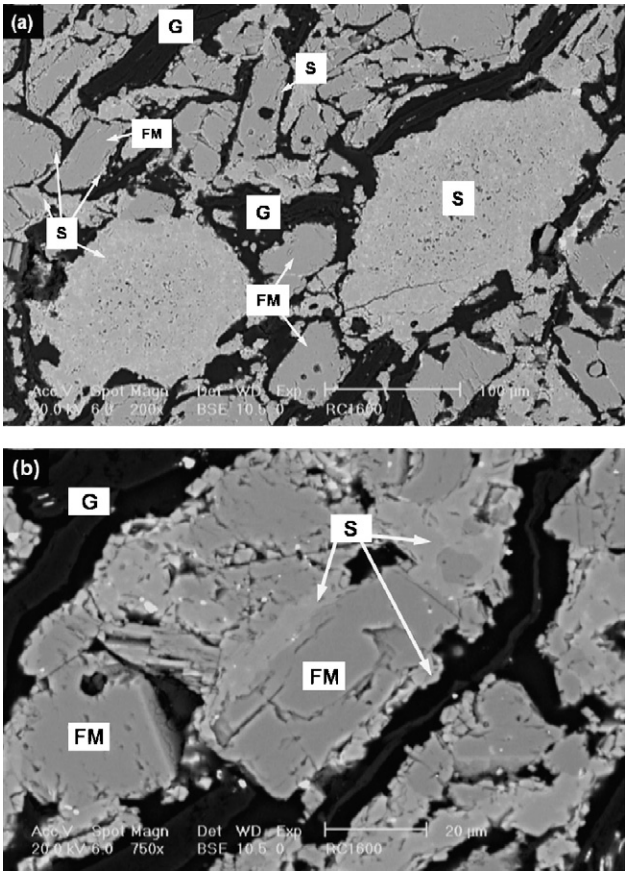

Fig. 11. SEM micrograph of the MRC sample fired at 1600 °C showing the solid spinel grains (a), bonding between MgO–MgO grains and MgO–graphite flakes (b). FM: fused MgO; S: spinel; G: graphite.

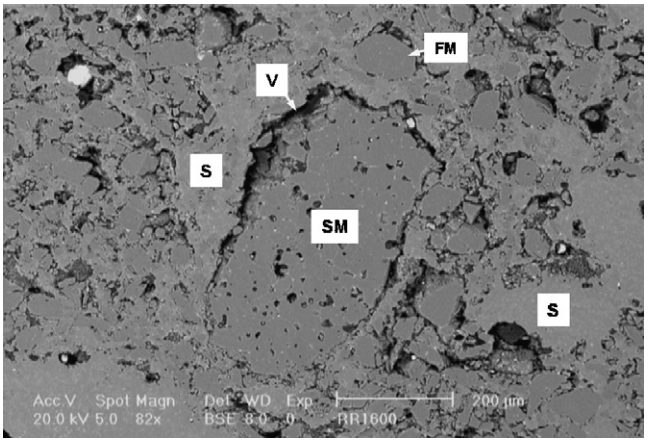

Fig. 13. SEM micrograph of the MRR sample fired at 1700 °C showing creation of void around of MgO grain. SM: sintered MgO; FM: fused MgO; S: spinel; V: void.

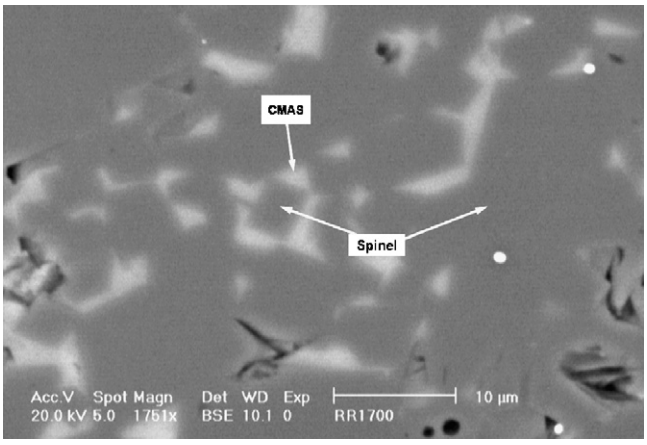

Fig. 14. SEM micrograph of the MRR sample fired at 1700 °C showing the spinel texture and trapped CMAS liquid phase in triple junctions.

the samples fired in the reducing atmosphere (MRC and MRR). The reasons of this phenomenon may be attributed to the spinel formation mechanism, as will be discussed as follows.

It is well known that MgO is not stable at high temperatures in the vicinity of carbon and solid–solid reaction between MgO and carbon at their interface results to the formation of $Mg_{(g)}$ (reaction (1)). According to the literatures [22,23], decomposition of $MgO_{(S)}$ occurs first (reaction (2)). The resultant oxygen is adsorbed at the surface of carbon and generates $CO_{(g)}$ (reaction (3)), which further reacts with $MgO_{(S)}$ to form $CO_{2(g)}$ and $Mg_{(g)}$ (reaction (4)).

$$MgO_{(S)} + C_{(S)} = Mg_{(g)} + CO_{(g)} \quad (1)$$

$$MgO_{(S)} = Mg_{(g)} + (1/2)O_{2(g)} \quad (2)$$

$$(1/2)O_{2(g)} + C_{(g)} = CO_{(g)} \quad (3)$$

$$CO_{(g)} + MgO_{(S)} = CO_{2(g)} + Mg_{(g)} \quad (4)$$

The partial pressure of $Mg_{(g)}$ and temperature play an important role on proceeding of reaction (1) to rightward in severe reducing atmosphere, which has been calculated by Yamaguchi [23] on the basis of JANAF data. He found that $MgO_{(S)}$ and $C_{(S)}$ exist as condensed phases in $P_{CO} = 1$ atm at 1600 °C and equilibrium P_{Mg} value is 0.18 atm. He also clarified the MgO–C reaction was started below 1400 °C and the rate is controlled by partial pressure of $Mg_{(g)}$ and $CO_{(g)}$ gases.

Therefore, $Mg_{(g)}$ in MCR and MRR samples created by carbothermal reaction of MgO could diffused into the area around the MgO surface and reacted with fine reactive alumina to form spinel. Consumption of $Mg_{(g)}$ dedicated to the spinel formation process usually forced the reaction (1) to proceed to the rightward. In fact, it could be concluded that the *in situ* spinel is formed in reactive alumina agglomerates according to the following mechanisms:

1. Solid-state reactions between MgO and Al_2O_3 on the surface of agglomerates at lower firing temperatures.
2. Solid–gas reactions between Al_2O_3 and $Mg_{(g)}$ in the center of agglomerates at higher firing temperature.

Therefore, the higher rate of solid–gas reaction and expansion behavior of *in situ* spinel formation in the center of agglomerates inhibit the hollow creation in the center of agglomerates in MRR and MRC samples (Figs. 10 and 12). However, in MRO sample, the *in situ* spinel formation was promoted by solid-state reaction where hollow spinel grains were formed in the original site of agglomerates (Fig. 7).

4. Conclusions

1. The *in situ* spinel formation due to reaction of reactive alumina and magnesia was detected to be initiated around 1000 °C in both reducing and oxidizing atmospheres. This reaction was completed above 1450 °C where no sign of the corundum peaks were found in the XRD patterns.
2. The partial pressure of $Mg_{(g)}$ originated from MgO reduction was found to have an important role on the *in situ* spinel formation. The solid–gas reaction is affecting partially the formation of solid spinel in MgO–C refractories.
3. The intermediate phases such as CA_6 were clarified to be formed due to reaction of MgO impurities with reactive alumina at 1450 °C. The low-melting CMAS phases was also formed in triple junction of spinel, which was believed to be responsible for corrosion resistance decrease at high temperatures.
4. The nature of spinel in MgO–C refractories matrix produces an interlocking texture, which holds the graphite flakes within and improves the structural integrity. In this type of skeleton structure, the graphite and antioxidants can be confidently increased for getting better wear resistance and with less negative effects on properties of MgO–C refractories.

Acknowledgment

We would like to thank research and development center of Pars Refractories Co. (PRC) for their financial and in-kind supports.

References

[1] G.C. Ulmer, Chromium spinel, in: A. M. Alper (Ed.), High Temperature Oxides. Part I. Magnesia, Lime and Chromium Refractories, New York, USA, 1970, pp. 252–315.
[2] H. Sarpoolaky, S. Zhang, W.E. Lee, Corrosion of high alumina and near stoichiometric spinels in iron-containing silicate slags, J. Eur. Ceram. Soc. 23 (2003) 293–300.
[3] W.E. Lee, P. Korgul, K. Goto, D.R. Wilson, Microstructural analysis of corrosion mechanisms in oxide-spinel steelmaking refractories, in: Advanced in Refractories for the Metallurgical Industries, Canada, 1996, pp. 453–465.
[4] D. Gutierez, J.I. Diaz, R.M. Rodriguez, Evolution of an alumina–magnesia/self-forming spinel castable. Part I. Microstructural features, Ceramica 45 (292) (1999).
[5] M. Bavand-Vandchali, F. Golestani-Fard, H. Sarpoolaky, H.R. Rezaie, C.G. Aniziris, The influence of in situ spinel formation on microstructure and phase evolution of MgO–C refractories, J. Eur. Ceram. Soc. 28 (2008) 563–569.

[6] S. Zhang, N. Marriott, W.E. Lee, Thermochemistry and microstructures of MgO–C refractories containing various antioxidants, J. Eur. Ceram. Soc. 21 (2001) 1037–1047.
[7] I. Ganesh, S. Bhattacharjee, B.P. Saha, R. Johnson, K. Rajeshwari, R. Sengupta, M.V.R. Rao, Y.R. Mahajan, An efficient $MgAl_2O_4$ spinel additive for improved slag erosion and penetration resistance of high-Al_2O_3 and MgO–C refractories, Ceram. Int. 28 (2002) 245–253.
[8] Z. Zhang, N. Li, Effect of polymorphism of Al_2O_3 on the synthesis of magnesium aluminate spinel, Ceram. Int. 31 (2005) 583–589.
[9] R. Sarkar, K. Das, S.K. Das, G. Banerjee, Development of magnesium aluminate spinel by solid oxide reaction, in: Proceedings of the UNITECR′97, USA, (1997), pp. 1053–1058.
[10] C. Aksel, P.D. Warren, Thermal shock parameters [R, R‴ and R⁗] of magnesia-spinel composites, J. Eur. Ceram. Soc. 23 (2003) 301–308.
[11] W.E. Lee, S. Zhang, H. Sarpoolaky, Different types of *in situ* refractories: fundamentals of refractory technology, Ceram. Trans. 125 (2001) 245–252.
[12] W.E. Lee, S. Zhang, M. Karakus, Refractories: controlled microstructure composites for extreme environments, J. Mater. Sci. 39 (2004) 6675–6685.
[13] P. Korgul, D.R. Wilson, W.E. Lee, Microstructural analysis of corroded alumina-spinel castable refractories, J. Eur. Ceram. Soc. 17 (1997) 77–84.
[14] H. Sarpoolaky, K.G. Ahari, W.E. Lee, Influence of *in situ* phase formation on microstructural evolution and properties of castable refractories, J. Eur. Ceram. Soc. 28 (2002) 487–493.
[15] M. Rigaud, S. Palco, N. Wang, Spinel formation in the MgO–Al_2O_3 system relation to basic castables, in: Proceedings of the UNITECR′95, 1995, pp. 384–394.
[16] Z.E. Nakagawa, N. Enomoto, I.S. Yi, K. Asano, Effect of corundum/periclase sizes on expansion behavior during synthesis of spinel, in: Proceedings of the UNITECR′95, 1995, pp. 379–386.
[17] S. Zhang, H.R. Rezaie, H. Sarpoolaky, W.E. Lee, Alumina dissolution into silicate slag, J. Am. Ceram. Soc. 83 (4) (2000) 697–903.
[18] M. Fuhrer, A. Hey, W.E. Lee, Microstructural evolution in self-forming spinel/calcium aluminate-bonded castable refractories, J. Eur. Ceram. Soc. 97 (1997) 813–820.
[19] D. Aza, A.H. Iglesias, J.E. Pena, Ternary system Al_2O_3–MgO–CaO. Part II. Phase relationship in the subsystem Al_2O_3–$MgAl_2O_4$–$CaAl_2O_7$, J. Am. Ceram. Soc. 83 (4) (2000) 919–927.
[20] W.E. Lee, S. Zhang, Melt corrosion of oxide and oxide-carbon refractories, Int. Mater. Rev. 43 (3) (1999) 77–104.
[21] W.E. Lee, S. Zhang, N. Li, B. Zhu, Microstructural characterization of *in situ* matrix phase formation in refractories, in: Proceedings of the UNITECR′01, 2001.
[22] T. Suruga, Effect of high temperature on MgO–C reaction, Taikabutsu Overseas 18 (4) (2000) 5–10.
[23] A. Yamaguchi, Thermochemical analysis for reaction process of aluminium and aluminium-compounds in carbon containing refractories, Taikabutsu Overseas 7 (2) (1987) 11–16.